PHYSICAL REVIEW B VOLUME 30, NUMBER 2 15 JULY 1984

Line defects in silicon: The 90° partial dislocation

James R. Chelikowsky
Corporate Research Science Laboratories, Exxon Research and Engineering Company, Annandale, New Jersey 08801

J. C. H. Spence
Department of Physics, Arizona State University, Tempe, Arizona 85287
(Received 5 December 1983)

We have examined the structural and electrical properties of an extended defect in silicon: the 90° partial dislocation. We present a detailed atomic geometry for this defect. The geometry was determined by using an approximate geometry from electron microscopy and by optimizing this approximate geometry to minimize strain energies. We have calculated the electronic states associated with the defect from the optimized geometry. We performed this calculation with a semiempirical pseudopotential and a peripheral-orbital method. We find, in qualitative agreement with experiment, two defect bands: One occupied band in the lower-half of the band gap and one empty band in the upper-half of the band gap. However, given the dispersion and weak localization of these bands, it is doubtful whether the bands correspond to those determined experimentally by either capacitance or photoconductive measurements. It is most probable that localized states occur at kinks or antiphase defects.

I. INTRODUCTION

The question of whether dangling bonds exist within the core of line defects in semiconductors is not a new one. Although the idea of dangling bonds along the core of the dislocation originated with Shockley[1] and Read[2] over 30 years ago, the actual existence of defect-associated dangling-bond states has yet to be resolved despite considerable effort. The motivation for this effort should be clear. Numerous properties of semiconductors depend on the nature of defect states. For example, models for recombination, luminescence, and lattice friction are strongly dependent on whether dislocations contain dangling bonds and on whether the defect states are deep or shallow.[3]

While the details of dangling-bond states associated with the dislocation cores have not been resolved, contemporary developments have brought us much closer to an answer. These developments include improved experimental techniques such as electron microscopy, cathodoluminenscence, temperature-dependent electron-beam-induced conductivity, and scanning deep-level transient spectroscopy.[4] In addition, new theoretical techniques for handling the electronic structure of defects have been developed. These techniques include those developed initially both for point and line defects.[5,6]

The aim of the experimental and theoretical work has been to determine the atomic and electronic structure of line defects. With respect to atomic structure, the situation is similar to that found in surface studies, i.e., no experimental technique now exists which can yield, in a routine fashion, accurate structures for nonperiodic, or partially periodic structures. This situation is likely to be improved, however, in the near future with the development of the scanning tunneling microscope and UHV transmission-electron microscopy.[7] For line defects, the experimental difficulties in obtaining structural and spectral information from a single isolated dislocation of known character and state of dissociation are considerable. The further separation of effects intrinsic to the dislocation core from those due to the decoration by impurities raises even more fundamental unresolved problems.

While first-principles theoretical techniques now exist which are applicable to line and planar defects, their implementation is by no means routine and, to date, no such calculations exist. For the electrical properties, current theoretical methods are adequate for spectroscopic determination, provided that accurate structural data exists. Thus, from a theoretical point of view, the chief difficulty in describing the line defect is the lack of structural information.

In this paper, we consider the structure and the electrical properties of the 90° partial dislocation in silicon. The low-temperature deformation of silicon and germanium produces predominantly dissociated screw dislocations (consisting of two 30° partial dislocations) and dissociated 60° dislocations (consisting of one 90° and one 30° partial), each with a total Burgers vector of the $(\frac{1}{2})[110]$ type on the (111) slip plane.[8] Dislocations running in other directions can be considered as kinked segments of these types. Thus, the fundamental dislocations are the 30° and 90° partial dislocations. We have dealt with the 30° partial elsewhere.[5] Here we concentrate on the 90° partial dislocation.

The 90° partial appears to be more difficult to describe than the 30° partial. A few calculations[8,9] exist which attempt to determine the atomic geometry of the core. While these efforts are in general agreement in suggesting that the 90° partial has a larger strain field associated with the core geometry as compared to the 30° partial dislocation, the detailed geometry has been somewhat controversial. It has been claimed[8] that the geometry is unstable and will not reconstruct when valence-force-field descrip-

 ©1984 The American Physical Society

tions using anharmonic contributions are considered. Others,[9] using similar methods, have suggested that it will strongly reconstruct (regardless of the precise nature of the valence force field). Independent of this controversy is the fact that neither calculation has presented explicit coordinates for the partial dislocations.

Another area of some controversy, involves the role of Peierls distortions. It is not clear whether a Peierls transformation is possible in this structure, although it has been suggested to be an important factor. In addition, the position of the theoretical defect bands for the 90° partial dislocation has not been decided conclusively. Moreover, experimental work on the 90° partial, while in reasonable agreement, has not yielded a consistent placement for the defect bands.

In this paper, we present for the first time an explicit set of atomic coordinates for the 90°-partial dislocation. We hope that these conditions will be the subject of an experimental verification when the state of the art allows the direct measurement of defect coordinates. Moreover, we present a new method for determining these coordinates. Our method is based on the use of a "mean-field" determination of the coordinates in a valence force field. Also, by using a semiempirical pseudopotential calculation to calculate the electronic structure we avoid the multiparameter tight-binding scheme used in previous discussions of these systems. Our results suggest that the 90° dislocation has, at best, weakly localized states and that any strongly localized states must occur at kinks or phase boundaries along the dislocation line.

II. ATOMIC COORDINATES OF THE 90° PARTIAL DISLOCATION

The atomic coordinates for the core of the 90° partial dislocation are not directly accessible. Nevertheless, it is possible to determine a reasonable geometry. We start by using near-atomic-resolution electron micrographs.[5,10] These experimental high-resolution micrographs suggest the geometry for the 90° partial indicated in Fig. 1. The geometry corresponds to the glide model for the 90° partial. The partial dislocation may lie on either the closely spaced (111) glide planes or the more widely spaced shuffle planes.[10-12] Based on recent experimental work[10] the glide model is favored and is the model upon which we shall concentrate. Unfortunately, the subangstrom details of the core-charge distribution on which the electronic structure depends are not resolvable using current electron microscopes, which, at best, reveal structural detail down to about 2 Å and which produce images depending sensitively on the electron-optical parameters and specimen thickness.

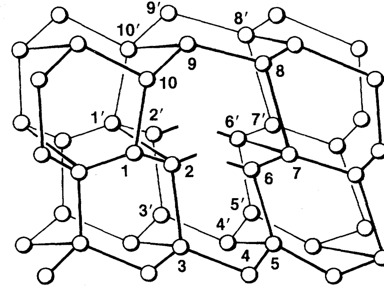

FIG. 1. Model of an unrelaxed 90° partial dislocation. The dislocation runs in the [110] direction. With no relaxation atoms 2,2′, and 6,6′ are not tetrahedrally coordinated.

To clarify our discussion we have numbered the atoms in the model shown in Fig. 1. The chief features of this configuration are that atoms 2 and 6 (or 2′ and 6′) are not tetrahedrally coordinated. The bond length is much larger than the crystalline bond length for silicon (e.g., ~10% larger than the ideal) and the bonding angles are far from the tetrahedral angle (e.g., ~165° as compared to 109.4°). In order to optimize this geometry we have allowed the atomic coordinates to relax. In doing so we have used a valence force field based on a modified Keating potential.[13] We use the expression given by Marklund[8] as derived by Koizumi and Ninomiya.[14] The elastic strain energy per atom is given by

$$E_{\text{atom}}=\frac{3\alpha}{16r_0^2}\sum_{i=1}^{4}(r_i^2-r_0^2)^2\exp\left[\frac{4\gamma\sqrt{3}}{3\alpha r_0}(r_i^2-r_0^2)^2\right]+\frac{3\beta}{8r_0^2}\sum_{\substack{i,j=1\\ i<j}}^{4}(\vec{r}_i\cdot\vec{r}_j+r_0^2/3)\exp\left[\frac{3\epsilon\sqrt{3}}{3\beta r_0}(\vec{r}_i\cdot\vec{r}_j+r_j^2-2r_0^2)\right]+\frac{\delta\sqrt{3}}{2r_0^3}\sum_{i=1}^{4}(\vec{r}_j\cdot\vec{r}_i+r_0^2/3)^3\,, \quad (1)$$

where r_0 is the crystalline bond length for silicon, $\vec{r}_i,\vec{r}_j$ are vectors connecting the specified atom with its four nearest neighbors, and α, β, γ, δ, and ϵ are parameters.[15] These parameters have been fit to the known elastic constants of silicon. The sums in Eq. (1) are over nearest neighbors. The expression attempts to incorporate both bond-stretching and bond-bending forces with a proper treatment of anharmonic terms. This description has some shortcomings, e.g., it predicts zero-stacking-fault energy (since a stacking fault involves second-nearest neighbors), the question of incomplete coordination is ambiguous, and the anharmonic terms may be overestimated. Nonetheless, we find that the resulting atomic coordinates are reasonable. Moreover, the errors we make in the geometry of this order are probably comparable to the errors arising elsewhere, e.g., our electronic structure calculations are based on semiempirical potentials which are not exact.

Before minimizing the energy expression in Eq. (1), given approximate coordinates from electron microscopy, we need to make a further approximation. Namely, we choose to confine our defect within an artificial superlattice. This configuration allows us to consider a finite system. We have considered two supercells: one with 24

atoms and one with 48 atoms. We would like to use as large a supercell as possible in order to minimize interactions between dislocations in the same and neighboring cells, yet small enough to allow accurate electronic structure calculations to be performed. We found that 24 atoms yielded a reasonable structure, but some discernable interactions between defects remained. Our 48-atom cell is probably the smallest cell which will yield accurate results. We embed two partial dislocations with opposite strain fields (i.e., Burgers vector) within the supercell. This results in a negligible strain field on the border of the unit cell. Moreover, it allows us to invoke inversion symmetry when obtaining a solution of Schrödinger's equation.

The optimization process is nontrivial as we wish to minimize the strain energy for each atom. Since we have 48 atoms in our unit cell, we would, in principle, have to consider a 144-parameter space minimization.[16] In order to make the problem tractable, we have proceeded in a mean-field manner. We first construct a matrix of fixed coordinates from the electron-microscopy work. The coordinates of a given atom were examined and an attempt was made to minimize the strain energy as given by Eq. (1). That is, using the forces derived from Eq. (1), we moved the atom within the fixed matrix to minimize the net force. After the given atoms' coordinates were altered, these coordinates were saved for future use and the procedure was repeated for another atom. When all the atoms in the matrix were examined, another matrix was set up with the saved coordinates and the process repeated. We constrain the atomic motions for each iteration to be small, e.g., typically 1% of the bond lengths. Thus, a number of iterations, typically ten, was performed until the coordinates converged. The advantages of this procedure are as follows. (a) It preserves the initial symmetry of the system. We need not be concerned with symmetry-breaking alterations of the coordinates as the atom moves in a fixed matrix which possess the correct symmetry. (b) It does not matter in which order the atomic coordinates are altered.

In Fig. 2 we present a model of the optimized 90°-partial-dislocation geometry. The key feature of our relaxed model is that all the atoms are now truly fourfold coordinated, i.e., all four neighboring atoms are within a few percent of the ideal bond length. However, some of the bond angles are considerably distorted from the tetrahedral angle. In Fig. 3 we present a projection of our unit cell with all 48 atoms indicated. The 90° partial dislocation is characterized by the intersection of a fivefold and sevenfold ring. The fivefold ring is composed of atoms 2-3-4-5-6-2 and the sevenfold ring contains atoms 1-2-6-7-8-9-10-1. This is a significant configuration as five- and sevenfold rings are thought to be a dominant component in amorphous semiconductors.[17] In Table I we give a tabulation of the coordinates for the 90° partial dislocation. We also give the strain energies as computed from Eq. (1).

The strain energies given in Table I must be considered approximate since the description of bond-bending and bond-stretching energies are approximate. With this caveat in mind, several features can be noted. First, the strain field falls off fairly rapidly. At a distance of two bond lengths away from the core atoms (2 and 6) the strain energy is reduced by an order of magnitude, e.g., atom 20 has a strain energy of 0.05 eV as compared to the 0.5-eV strain energy at the core. It is clear that some of this rapid decrease may be an artifact of the imposed inversion symmetry of the two partials within the supercell. However, similar results were obtained for the core-strain energies for the 24-atom unit cell. In any event, the

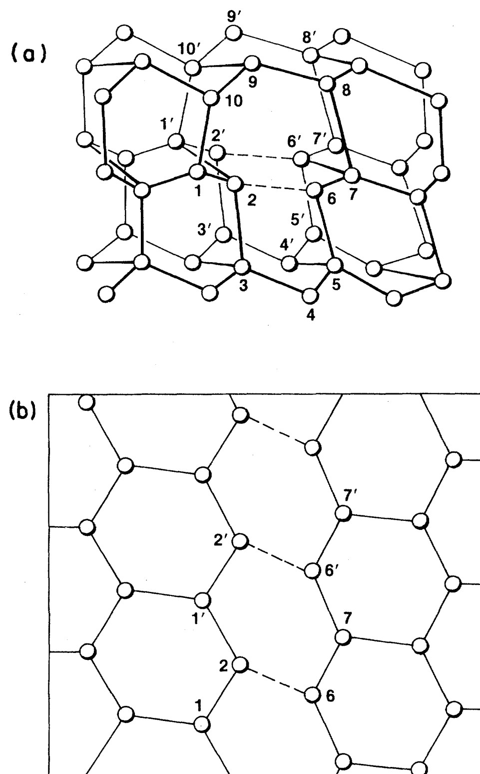

FIG. 2. (a) Diagrammatic sketch of a relaxed 90° partial dislocation. In this model, atoms 2,2' are allowed to bond to 6,6' to form fivefold (2-3-4-5-6-2) and sevenfold rings (2-6-7-8-9-10-1-2). (b) Projection of the atomic double layer containing atoms 1-2-6-7-7'-6'-2'-1. Note how the sixfold ring (1'-2-6-7-6'-2'-1') is significantly distorted from the bulk crystalline configuration.

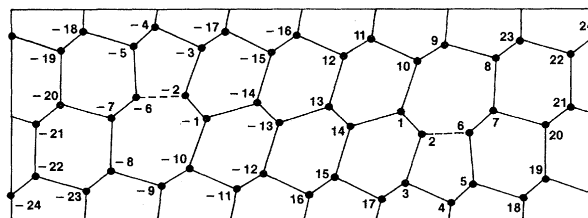

FIG. 3. Projection of the atomic positions listed in Table I onto a plane perpendicular to the line-defect direction. This supercell contains two 90° partial dislocations. Atom n is related to atom $-n$ by inversion through the origin. Atoms 2,6 or $-2, -6$ are located at the dislocation core. The extra half-plane of atoms contains 4,5,6.

TABLE I. Atomic coordinates (in Å) of the relaxed 90° partial dislocation within a supercell configuration. There are two dislocations in the supercell with a center of inversion at the origin. The numbering of the atoms is the same as in Fig. 3. The supercell is an orthorhombic cell with the following dimensions: $a=26.11$ Å, $b=9.40$ Å, $c=3.84$ Å, $\alpha=90°$, $\beta=90°$, and $\gamma=90°$. The strain energy (in eV/atom) from a valence field force, Eq. (1), is also given.

Atom	X	Y	Z	E
1	4.37	0.10	2.31	0.20
2	5.29	−0.85	0.47	0.50
3	4.59	−3.04	0.13	0.27
4	6.63	−3.95	−0.07	0.18
5	7.61	−3.09	1.81	0.11
6	7.43	−0.82	1.44	0.48
7	8.55	0.10	−0.39	0.12
8	8.59	2.46	−0.12	0.05
9	6.31	3.13	0.04	0.14
10	5.08	2.36	2.01	0.20
11	2.97	3.32	1.99	0.06
12	1.79	2.60	0.06	0.13
13	1.14	0.33	0.09	0.14
14	2.09	−0.54	2.04	0.15
15	1.43	−2.80	1.97	0.14
16	0.29	−3.56	0.02	0.11
17	3.48	−3.79	2.04	0.08
18	9.82	−3.74	1.85	0.05
19	10.85	−2.86	−0.06	0.01
20	10.82	−0.52	−0.11	0.05
21	11.93	0.33	1.83	0.03
22	11.95	2.68	1.89	0.02
23	9.69	3.32	1.82	0.05
24	13.03	3.53	−0.02	0.02

strain-field perturbation on the atomic coordinates is expected to be of longer range than the range of significant perturbation on the electronic structure. With respect to the magnitude of the strain energies, the core strain is not small; however, it is in accord with typical surface energy strains.[19] Unlike the work of Marklund,[8] but in accord with the results of Lapiccirella and Lodge,[9] we do find a stable configuration with the force field of Koizumi and Ninomiya.[16] In fact, our final configuration is somewhat similar to the one Marklund obtained with the Keating potential. In Table II we compare our bond lengths and angles to his work. The largest differences from Marklund's work is on the order of 1%; the bond angles differ by a few degrees. In fact, the differences in our bond angles from Marklund's, e.g., the angles subtended by atoms 1′-2-6 and 7-6′-2′ as in Fig. 2, arise from some asymmetry resulting from our supercell configuration rather than an intrinsic feature of the defect. (It was necessary to distort some of the bond lengths and angles to create a periodic structure.) We view the differences, i.e, typically 1% in the bond length and 3° in the bond angle, to be well within the uncertainties of force-field descriptions.

TABLE II. Comparison between structure determined by present method to that calculated by Marklund (Ref. 8). The atoms are numbered as in Fig. 3. Bond lengths are given in terms of the experimental bond length of crystalline silicon ($r_0=2.35$ Å).

Bonding atoms	Present model	Ref. 7
	Bond length	
2-6	$1.00r_0$	$1.01r_0$
1′-2	$1.02r_0$	$1.03r_0$
1-2	$0.97r_0$	$0.97r_0$
	Bond angles	
1′-2-6	133.7°	135.0°
1-2-6	91.7°	95.5°
7-6-2	96.2°	95.3°
7-6′-2′	138.2°	135.0°

III. ELECTRONIC STRUCTURE OF THE 90° PARTIAL DISLOCATION

A. Computational methods

Given the atomic coordinates in Table I we have performed a numerical solution of the one-electron Schrödinger equation to determine the existence of any localized states. For the 30° partial, we found[5] that the reconstructed defect resulted in no localized states. However, here the deviations in bond lengths and angles (in contrast to the 30° partial) are sufficiently large so that localization of states along the defect core is possible.

Owing to the size of our unit cell, and to uncertainties in the atomic coordinates, a fully-self-consistent treatment of the 90° partial dislocation was not performed. Instead, we used a semiempirical potential for silicon determined from atomic, bulk, and surface considerations. The construction follows the work of Kane.[18] The form of the potential is taken to be

$$V(\vec{r})=\sum_{\vec{R},\vec{\tau}_\mu} V^a(\vec{r}-\vec{R}-\vec{\tau}_\mu)\,,$$
$$V^a(r)=\sum_{i=1}^{2} a_i\exp(-\beta_i r^2)\,, \tag{2}$$

where $\vec{R}$ is a lattice vector, the parameters a_i and b_i are given in Table III, and $\vec{\tau}_\mu$ locates the atomic sites in the unit cell. We have assumed that this potential is transferable from the crystalline site to a defect site. In order to test the transferability of the potential, the Si(111) surface has been computed by using the potential at both bulk and surface sites.[5] No significant differences were found between this method and a fully-self-consistent treatment,[5] i.e., the surface bands determined by the two procedures differed by less than ~0.2 eV.

The basis functions we use for the solution of

TABLE III. Potential parameters (a_i and b_i) as defined by Eq. (2). a_i is in units of rydbergs and b_i is in units of (a.u.)$^{-2}$.

a_i	b_i
−7.744	0.38
10.362	0.76

Schrödinger's equation are expanded in Gaussians; with the potential in Eq. (1) expressed in Gaussians, all the matrix elements required can be evaluated analytically. The basis functions we employ are of the form

$$\Phi_{\mu,\nu}(\vec{k},\vec{r})=\sum_{\vec{R}}\exp[i\vec{k}\cdot(\vec{R}+\vec{\tau}_\mu)]f_\nu(\vec{r}-\vec{R}-\vec{\tau}_\mu)\ , \tag{3}$$

where ν indicates the orbital type. The f_ν are given by

$$f_\nu(\vec{r})=g_\nu(\vec{r})\exp(-\alpha r^2)\ , \tag{4}$$

where g_ν are polynomials of s, p, and d symmetry. We use two s-like orbitals,[20] three p-like orbitals, and five d-like orbitals per atom. The decay constant α was set equal to 0.186 as suggested by Kane.[18] Our method differs significantly from other approaches, e.g., Marklund,[21] in that we calculate the Hamiltonian matrix elements without recourse to an empirical scaling formula or extensive parametrization.

With ten orbitals per atom and 48 atoms in our supercell, we would need to diagonalize a 480$\times$480 matrix. While a matrix of this size can be handled with contemporary computers, we employ Louie's method of peripheral orbitals[22] to reduce the matrix size by a factor of 2. Louie has shown that by properly treating the s, p, and d orbitals, one may treat the d orbitals in a modified form of Lowdin's perturbation theory. In this method, only the s- and p-orbital contributions are handled directly; the d-orbital contribution is treated in a perturbative fashion. Hence, our Hamiltonian matrix reduces to a 240$\times$240 matrix. The computational time is reduced concurrently for the diagonalization process.

B. Results and discussion

By summing over all occupied states we can determine the valence charge density surrounding the partial dislocation. This charge density is obtained from a Fourier expansion of the Gaussian orbitals. We can use the density to give an impression of the bonding associated with the defect and to obtain a qualitative picture of the magnitude of the perturbation of the dislocation on the crystalline properties. In Fig. 4 we present the calculated valence charge density for the (110) plane containing the defect core. It is apparent that some significant distortion from the ideal crystalline charge density exists. The bonds within the core of the defect are decidedly weaker in terms of the magnitude of the bonding charge, i.e., the maximum charge density along the bonding direction is considerably reduced from its bulk value. Moreover, the fluctuations in the charge density are smaller than the bulk; the charge density is more uniform and, hence, more metallic. While the perturbation is significant, the extent of the dislocation's disruption on the bonding is fairly short ranged. We have allowed seven bond lengths between core atoms within the supercell; the perturbation appears to "heal" by this distance. We also note that the density is not ideal away from the defect. This is a result of the strain field and small deviations from the tetrahedral bonding angles and from the ideal bond lengths.

By examining the degree of localization of each state

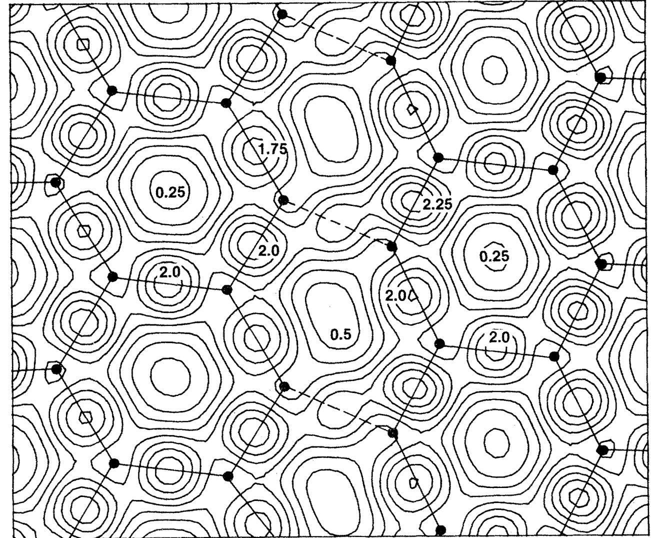

FIG. 4. Total valence charge density for the 90° partial dislocation. For the purposes of constructing the density, we have summed over the densities in several planes, averaged it, and plotted it in the (111) x-y plane. In this manner we may compare the density to the atomic positions in Fig. 2(b). The contour spacing is in units of 0.25 with the charge normalized to one electron in the unit cell. The plane of the page is (111) and the vertical axis runs in a [110] direction.

within the defect core, it is possible to determine the nature of the defect bands associated with the dislocation. Owing to the significant perturbation of the total charge, we expect that defect bands may exist within the optical

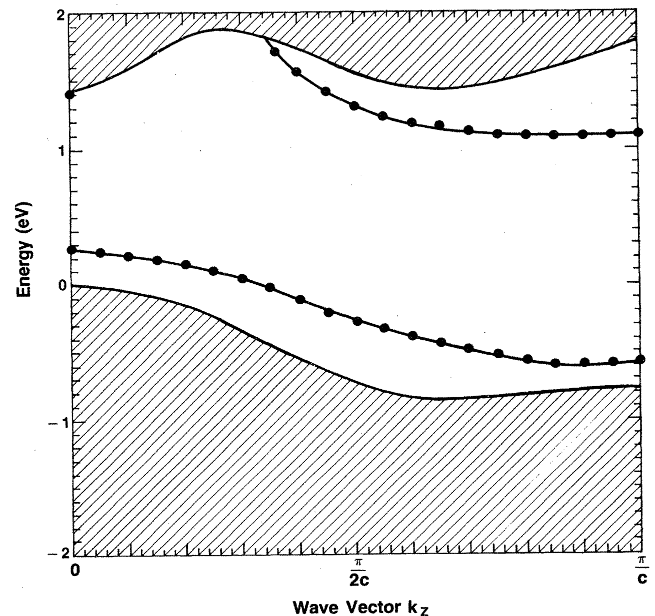

FIG. 5. Energy-band spectrum of the dislocation states and the projected crystalline band structure. The top of the valence band is taken to be the zero reference. Two defect bands intrinsic to the 90° partial dislocation are indicated in the band gap. The lower band is completely occupied; the upper band is empty.

gap of silicon. In Fig. 5 we present defect energy bands for the dislocation. We find two bands: one occupied and near the top of the valence band, and one empty and near the bottom of the conduction band. We find a gap of about 0.7 eV between the bands. Thus we find that the bonding along the dislocation is semiconducting as opposed to metallic. The perturbation of the dislocation, while weakening the bonds, does not result in unsaturated bonding.

Both defect bands are weakly localized near the zone center and become most strongly localized at the zone edge. The empty band clearly becomes resonant with the bulk states near the zone center. We can follow it for several electron volts above the valence band before it becomes essentially a bulklike state. The interaction between the two defects within our supercell lifts the double degeneracy of the defect bands, i.e, if the supercell were of infinite extent and we separated the two partial defects by an infinite amount, we would expect two degenerate bands for each defect band. For the case at hand, the degeneracy is lifted by about $\sim$0.3 eV. For the sake of clarity, we have illustrated the center of mass of the defect-defect—interaction—split bands.

Our results appear consistent with experiment[4,23] in that we find a semiconductorlike behavior along the dislocation. If we had found metalliclike behavior, i.e., fractionally occupied bands, then one would expect the possibility of a strong spin signal in resonance experiments. This has not been observed. It has been suggested that filled and empty defect bands exist along the dislocation.[23] While this is in accord with our theory, it is by no means clear that the bands we find are in agreement with the experiments. First, the gap we find and the quantitative placement of the bands seems at variance with those proposed by Mergel and Labusch.[23] Second, the bands we find are fairly broad. The occupied band has a width of about 1.4 eV and the empty band one of at least 1.0 eV. It is doubtful that such bands could produce the sharply defined features observed. This conclusion has also been reached by Jaros and Kirton[24] on the basis of their examination of how dangling bonds interact in crystalline silicon. They argue that dangling bonds associated with line defects will always result in defect bands broader than those observed by capacitance measurements. A more likely origin of defect-associated states is from extrinsic effects such as impurities or from kinks along the defect. Another possibility is the existence of dangling-bond states at antiphase boundaries, i.e., antiphase defects. A complete description of the antiphase defect is given by Hirsch.[25] These defects correspond to a phase-boundary dangling bond which exists between regions of different relaxation symmetries. For example, it is possible for relaxation to occur where bonds from atom 2 exist with equal probability to atom 6 or to atom 6′. Domains may exist where 2-6 bonding regions adjoin 2-6′ bonding regions. In these regions, atom 2 may have neighbor atoms (6 and 6′) which are fully coordinated; atom 2 would exhibit a dangling bond which corresponds to an antiphase defect. It should be possible for this dangling bond to propagate along the dislocation line and to form a soliton-like disturbance. We expect this possibility to be greater for the 90° partial dislocation than for the 30° partial dislocation based on the greater strain field which we find for the 90° than for 30° partial. Moreover, we find that the 30° partial does not form localized states as does the 90° partial. This suggests the bonds along the 90° partial are weaker and that dangling-bond propagation is more likely.

It has been proposed that the 90° partial undergoes a Peierls-type structural transition.[23,26] We find no evidence for this possibility in that the bonding along the defect is saturated. If we had found our valence-force-field model could not yield a saturated configuration for the 90° partial dislocation, a classical Peierls model would be appropriate as the dangling-bond band would be half-filled. Moreover, Altman[27] has noted that the periodicity along the line defect does not double upon rebonding. Thus, he argues that a Peierls model, while appropriate for the 30° partial dislocation, is not appropriate for the 90° partial dislocation.

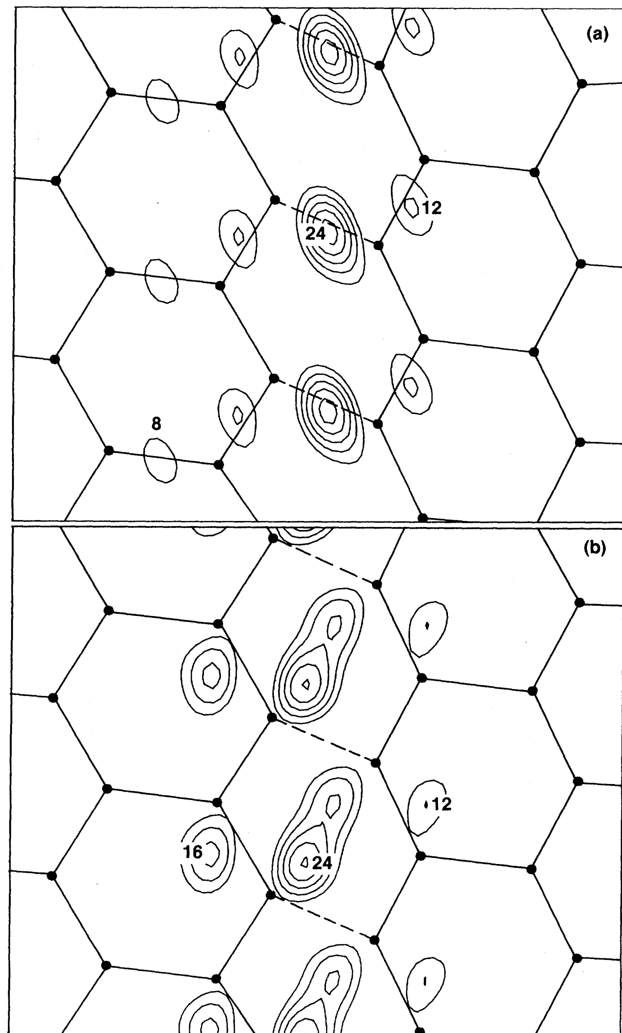

FIG. 6. Charge density of two dislocation states at the zone edge ($k_z=\pi/c$). The contour spacing is in units of 4.0. The charge is normalized to one electron per unit cell ($\Omega_c=942.47$ Å^3). (a) Occupied defect-band-state charge density. (b) Empty defect-band-state charge density. Directions as for Fig. 4.

By considering the wave functions for the defect bands, we may plot out the probability densities for these bands. The probability densities (or in the case of the occupied band, the charge density) give (gives) information on the origin of the defect bands. The densities are illustrated in Fig. 6 for the empty and occupied bands. The wave functions were taken at the zone edge where the bands are most localized; however, away from the zone edge, the states are quite similar, but less localized at the defect core. We find that a rather simple interpretation can be made for these defect states. Consider the case before any relaxation. Suppose we examine atom 2, although the discussion would hold equally well for atom 6. Initially, before relaxation, atom 2 will be equidistant from atoms 6 and 6′. The bond lengths, however, are about 10—15 % greater than the ideal length. As we relax the atomic positions and move atom 2 toward atom 6, a bond will start to form between atoms 2 and 6. If we were to form a perfect crystalline bond, no defect state would exist. However, the 2-6 bond is not perfect and does not result in a state which merges with the bulk continuum. This is the origin of the occupied band. The distance between atom 2 and atom 6′ is such that a bond does not form; however, this interaction is significant enough to localize an empty band below the conduction-band minimum.

It should be possible to excite states from the occupied defect band into the empty band. Although we have not calculated a dipole matrix element, from Fig. 6 it appears that a significant overlap can occur. We also note that the direction of the dipole should be along the dislocation line.[28] This result is consistent with recent cathodoluminescence measurements from individual dislocations of a known Burgers vector is diamond.[29] However, luminescence polarized along the dislocation-line direction has also been observed from screw dislocations (which consist of two 30° partials), so that another mechanism is also possible. Decoration by donor-acceptor pairs of variable spacing along the dislocation line has been proposed[29] to account for the polarization result and large observed emission linewidth, but has not been considered here for silicon. An experimental test of the model described here will be possible in the near future when the infrared luminescence which has been identified as arising from dislocations in silicon[30] is obtainable from individual well-characterized dislocations in correlation with a transmission-electron-microscope image.

ACKNOWLEDGMENTS

One of us (J.C.H.S.) would like to acknowledge support from the National Science Foundation (NSF) Grant No. DMR-80-02108-04 and the facilities of the NSF National High Resolution Electron Microscopy Center at Arizona State University.

[1] W. Schockley, Phys. Rev. **91**, 228 (1953).

[2] W. T. Read, Jr., Philos. Mag. **45**, 775 (1954).

[3] A general review of the electronic structure of dislocations in tetrahedrally coordinated semiconductors can be found in J. Phys. (Paris) Colloq. **40**, C6 (1979), and in the forthcoming Proceedings of the International Conference on Dislocations in Semiconductors, Aussois, 1983 [J. Phys. (Paris) Colloq. (in press)] on the same topic.

[4] Representative experimental papers include the following: L. C. Kimerling and J. R. Patel, Appl. Phys. Lett. **34**, 73 (1979); P. B. Hirsch, J. Microsc. (Oxford) **118**, 3 (1979); D. Mergel and R. Labusch, Phys. Status Solidi B **114**, 545 (1982); N. Yamamoto, J. C. H. Spence, and D. Fathy, Philos. Mag. (to be published).

[5] J. E. Northrup, M. L. Cohen, J. R. Chelikowsky, J. C. H. Spence, and A. Olsen, Phys. Rev. B **24**, 4623 (1981); J. R. Chelikowsky, Phys. Rev. Lett. **49**, 1569 (1982).

[6] J. Bernholc and S. T. Pantelides, Phys. Rev. B **18**, 1780 (1978); J. Bernholc, N. O. Lipari, and S. T. Pantelides, *ibid.* **21**, 3545 (1980); G. A. Baraff and M. Schlüter, Phys. Rev. Lett. **41**, 892 (1978); Phys. Rev. B **19**, 4965 (1979).

[7] A review of new techniques for surface-structure analysis (including scanning tunneling microscopy and UHV surface transmission electron microscopy) can be found in Proceedings of the Wickenburg Conference on Surface Science, 1983, edited by O. L. Krivanek (unpublished).

[8] S. Marklund, Phys. Status Solidi B **100**, 77 (1980).

[9] A. Lapiccirella and K. W. Lodge, in *Microscopic Semiconductor Materials Conference, Oxford, 1981* (IOP, London, 1981), p. 51.

[10] A. Olsen and J. C. H. Spence, Philos. Mag. A **43**, 945 (1980).

[11] K. Wessel and H. Alexander, Philos. Mag. **35**, 1523 (1977).

[12] J. P. Hirth and J. Lothe, *Theory of Dislocations* (McGraw-Hill, New York, 1968).

[13] P. N. Keating, Phys. Rev. **145**, 637 (1966); **149**, 674 (1966).

[14] H. Koizumi and T. Ninomiya, J. Phys. Soc. Jpn. **44**, 898 (1978).

[15] The parameters we use are given by $\alpha=0.8477$, $\beta=0.2412$, $\gamma=-0.162$, $\delta=0.021\,735$, and $\epsilon=-0.0652$. With these parameters the energy per atom is in electron volts.

[16] Actually, if we demand that our unit cell have inversion symmetry, we need to consider a 72-parameter space optimization.

[17] See, for example, the review by J. D. Joannopoulos and M. L. Cohen, in Solid State Phys. **31**, 71 (1976).

[18] E. O. Kane, Phys. Rev. B **13**, 3478 (1976).

[19] D. J. Chadi (private communication).

[20] Two s orbitals are used in our work. One s orbital is nodeless; the other is not and corresponds to an excited s state with the form $r^2\exp(-\alpha r^2)$. We find that an excited s-type state must be included to replicate the lower conduction bands.

[21] S. Marklund, Phys. Status Solidi B **85**, 673 (1978); **92**, 83 (1979).

[22] S. G. Louie, Phys. Rev. B **22**, 1933 (1980).

[23] D. Mergel and R. Labusch, Phys. Status Solidi B **114**, 545 (1982).

[24] M. Jaros and M. J. Kirton, Philos. Mag. B **46**, 85 (1982).

[25] P. B. Hirsch, J. Microsc. (Oxford) **118**, 3 (1979).

[26] R. Jones, in Microscopy of Semiconducting Materials (unpublished), p. 45.

[27] S. L. Altman, J. Phys. C **15**, 907 (1982).

[28] As noted in the text, owing to our use of supercells, we introduce some artificial strain asymmetry around the defect. This affect accounts for some of the asymmetry in the bonding

charge in Fig. 6. Also, the plane we plot in is a projection of the charge and this projection may also introduce some asymmetry.

[29]N. Yamamoto, J. C. H. Spence, and D. Fathy, Philos. Mag. (to be published).

[30]J. Weber, R. Sauer, E. R. Weber, and H. Alexander, Phys. Status Solidi (to be published). See also E. R. Weber and H. Alexander, in Proceedings of the International Conference on Dislocation in Semiconductors, Aussois, 1983 [J. Phys. (Paris) Colloq. (in press)].